Composite Structures 293 (2022) 115728

Contents lists available at ScienceDirect

Composite Structures

journal homepage: www.elsevier.com/locate/compstruct

Heat transfer analysis in multi-layered materials with interfacial thermal resistance

Wei-bin Yuan [a], Nanting Yu [b,*], Long-yuan Li [b], Yuan Fang [c]

[a] College of Architecture and Civil Engineering, Zhejiang University of Technology, Hangzhou 310023, China
[b] School of Engineering, Computing and Mathematics, University of Plymouth, Plymouth, Devon PL4 8AA, UK
[c] Guangdong Provincial Key Laboratory of Durability for Marine Civil Engineering, Shenzhen University, Shenzhen 518060, China

ARTICLE INFO

Keywords:
Heat transfer
Multilayer
Composites
Interfacial thermal resistance
Thermal barrier coatings

ABSTRACT

Interfacial thermal resistance (ITR) presents a measure of the thermal resistance to heat transport caused by the interface in composites to a thermal movement when the heat flows across it. In the heat transfer analysis, the presence of an ITR invalidates the continuity condition of temperature at the interface, so that a special treatment is required. In this paper, two one-dimensional models are developed for the heat transfer analysis in multi-layered materials with ITR. One is to create a virtual layer at the interface to represent the ITR and the other is to use a local artificial layer surrounding the interface with modified thermal properties to reflect the influence of ITR on the heat transfer in the layer involving the interface. As the application of the present models, numerical examples are also provided for the heat transfer analysis of a multi-layered composite and a substrate with multilayer surface coatings, from which the effect of ITR on the heat transfer in composite materials is demonstrated.

1. Introduction

Composites with multilayer materials, due to their outstanding thermal, electrical, chemical and mechanical properties, have been widely used in civil, mechanical, aeronautical and aerospace engineering. A multi-layered composite normally consists of two or more layers of different materials with different chemical and/or physical properties. When they are combined, the jointed composite can produce the properties that are different from those of their original components. By changing the components and/or thicknesses of the layers one can produce the tailor-made properties of composite materials and/or composite structures. Typical examples of the multi-layered composites include the sandwich beams [1] made by attaching two thin but stiff skins to a light weight but thick core, which can produce high bending stiffness but have overall low density; the composite laminates [2] assembled of layers of fibrous composite materials, which are integrated together to provide required engineering properties such as bending stiffness, in-plane stiffness, strength and coefficient of thermal expansion; and the multilayer surface coatings [3] which combine the several materials of attractive properties, each chosen to solve a problem in the application to protect the substrate materials.

In recent years, there is a growing interest to use multi-layered composites to provide thermal barriers in structural components [4]. For instance, Srivastava et al. [5] proposed a three-layer coating architecture to reduce the heat transfer and chemical diffusion in die steel. Josell et al. [6] investigated the heat transfer through thermal barrier coatings (TBCs) composed of nanoscale thick layers. Kovalev et al. [7] analysed the physical nature of thermal barrier properties of nano-laminated films by using X-ray photoelectrons and high-resolution electron-energy loss spectroscopies. Tang et al. [8] developed a numerical model for turbine blades with TBCs and analysed the temperature distribution and thermal-stress field in different service stages. Liu et al. [9] reported a study on the TBCs insulation and the resultant stresses in coated blades. Zhu et al. [10] developed a three-dimensional finite element analysis model for turbine blades coated with multilayer-structured TBCs. Sun et al. [11] presented an experimental investigation on the thermal effect in picosecond laser drilling of thermal barrier coated In718. Ge et al. [12] reported an experimental investigation on the thermal radiation and conduction in functionally graded TBCs. Munuhe et al. [13] proposed an integrated model by incorporating simultaneous droplet spreading, wetting interactions, heat transfer, and liquid infiltration with temperature-dependent viscosities in unsaturated porous media. In literature, there are reports on the thermal resistance generated at the interface [14,15], particularly when the

* Corresponding author.
E-mail address: nanting.yu@plymouth.ac.uk (N. Yu).

https://doi.org/10.1016/j.compstruct.2022.115728
Received 30 January 2022; Received in revised form 1 April 2022; Accepted 8 May 2022
Available online 12 May 2022
0263-8223/© 2022 The Author(s). Published by Elsevier Ltd. This is an open access article under the CC BY license (http://creativecommons.org/licenses/by/4.0/).

materials on the two sides of the interface have significantly different thermal properties and/or the thickness of one of the layers involved is very thin. For example, Choi et al. [16,17] reported the influence of interphase characteristics on the thermal conductivity of carbon nanotubes reinforced polymer composites. Hassanzadeh-Aghdam et al. [18] examined the effect of surface coating of carbon nanotubes on the effective thermal conductivity of unidirectional polymer hybrid nanocomposites. Fang et al. [19] developed an analytical model to calculate the effective thermal conductivity with considering the interfacial thermal resistance (ITR). Note that the heat transfer analysis for the composites with multilayer materials is generally carried out by using numerical methods such as finite element methods, in which the temperature and heat flux are treated as the continuous functions in the formulations of finite element analysis. To deal with the ITR, one has to use special interface elements which are similar to the "contact elements" used in the structural analysis to deal with the discontinuity in displacement at the interface between the two involved materials in a composite structure [20]. The difficulty in developing such special interface elements is the formulation of governing equations to describe the discontinuity of physical variables and the determination of corresponding material constants to be used in the interface element. Currently, the ITR could be handled by using the interphase elements in which a liquid phase is artificially added at the interface with specified ITR. The liquid phase discontinues the materials on the two side of the interface and thus allows for the discontinuity of temperature at the interface. However, the use of such interphase elements not only requires the finite element model utilised to have a built liquid phase but also makes the element mesh inconvenient and increases the computational complexity.

ITR represents a measure of the thermal resistance provided by the interface to thermal transport when the heat flows across it. ITR arises because of the differences in the material properties on the two sides of the interface [21], and it results in a temperature jump at the interface whereas the continuity of heat flux is maintained there. The problem related to ITR was addressed as early as 1941 when Kapitza [22] discovered the temperature jump at an interface between solid and liquid phases. The similar phenomenon was also reported for the interface jointed by two solid materials [23–25]. In order to take account into the effect of ITR on the heat transfer in multilayer composite structures, various analysis models have been developed. One of the approaches is to modify the thermal properties of the materials in the two layers surrounding the interface to reflect the influence of ITR on the heat transfer [6,26]. This kind of approaches not only have some difficulty in determining the equivalent thermal properties but also may lead to inaccurate results because it dilutes the local effect of ITR. In this paper, two one-dimensional models are developed for the heat transfer analysis in the composites with multilayer materials in which the ITR is considered locally. One is to create a virtual layer at the interface to represent the ITR and the other is to use a local artificial layer surrounding the interface with modified thermal properties to reflect the influence of ITR on the heat transfer in the layer involving the interface. As the application of the present models, numerical examples are also provided for the heat transfer analysis of a multi-layered composite and a substrate with multilayer surface coatings, from which the effect of ITR on the heat transfer in composite materials is highlighted.

2. Description of heat transfer analysis in multi-layered composites with ITR

Consider a composite with multilayer materials, in which each layer can be treated as a homogeneous material. The governing equation for the heat transfer analysis of the composite is well known and can be expressed as follows,

$$(\rho_i c_i)\frac{\partial T_i}{\partial t} = \nabla(k_i \nabla T_i) \quad \text{in} \quad \Omega_i \,(\mathrm{i} = 1, 2, \cdots) \tag{1}$$

where ρ_i is the density, c_i is the specific heat, T_i is the temperature, t is the time, k_i is the thermal conductivity coefficient, Ω_i is the layer domain, and the subscript i represents the i-th layer. For a multi-layered composite two additional equations are required at each interface to define the temperature and heat flux, which can be expressed as follows [19,26],

$$k_i \frac{\partial T_i}{\partial n} = \frac{1}{R_{i,i+1}}(T_{i+1} - T_i) \quad \text{on} \quad \Gamma_{i,i+1} \,(\mathrm{i} = 1, 2, \cdots) \tag{2}$$

$$-k_{i+1}\frac{\partial T_{i+1}}{\partial n} = \frac{1}{R_{i,i+1}}(T_{i+1} - T_i) \quad \text{on} \quad \Gamma_{i,i+1} \,(\mathrm{i} = 1, 2, \cdots) \tag{3}$$

where n is the normal of interface, $R_{i,i+1}$ is the thermal resistance of the interface, and $\Gamma_{i,i+1}$ is the interface between layer i and layer i + 1. It is obvious from Eqs. (2)–(3) that, if there is no ITR, i.e. $R_{i,i+1} \to 0$, then Eqs. (2) and (3) reduce to the conventional continuity conditions for temperature and heat flux at the interface, i.e. $T_i = T_{i+1}$ and $k_i\frac{\partial T_i}{\partial n} = -k_{i+1}\frac{\partial T_{i+1}}{\partial n}$.

Theoretically, Eqs. (1)–(3) plus the initial and boundary conditions can be used to determine the temperature distribution in the multi-layered composite at any time. For instance, if the temperatures at a time t_k at three points x_{j-2}, x_{j-1}, and x_j are known (see Fig. 1), then the temperature at the time t_{k+1} at point x_{j-1} can be calculated from Eq. (1) by using the finite difference method with an explicit time integration scheme as follows,

$$T_p^{k+1} = T_p^k + \left(\frac{k_1}{\rho_1 c_1}\right)\left(\frac{\Delta t}{\Delta x^2}\right)\left(T_{p+1}^k - 2T_p^k + T_{p-1}^k\right) \quad (p = 2, 3, \cdots j-1) \tag{4}$$

$$T_p^{k+1} = T_p^k + \left(\frac{k_2}{\rho_2 c_2}\right)\left(\frac{\Delta t}{\Delta x^2}\right)\left(T_{p+1}^k - 2T_p^k + T_{p-1}^k\right) \quad (p = j+1, J+2, \cdots m-1) \tag{5}$$

where Δt is the increment of time t, Δx is the increment of coordinate x, (ρ_1, c_1, k_1) and (ρ_2, c_2, k_2) are the density, specific heat, and thermal conductivity coefficient in the layers 1 and 2, respectively, and T_p^k is the temperature at time t_k and coordinate point x_p. The temperatures at the two sides of the interface where $x = x_j = x_{j^*}$ can be calculated using Eqs. (2) and (3), which are given as follows,

$$T_j^{k+1} = \frac{\left(1 + \frac{\Delta x}{R_{1,2}k_2}\right)T_{j-1}^{k+1} + \frac{\Delta x}{R_{1,2}k_1}T_{j+1}^{k+1}}{1 + \frac{\Delta x}{R_{1,2}k_1} + \frac{\Delta x}{R_{1,2}k_2}} = \frac{\left(\frac{R_{1,2}}{\Delta x} + \frac{1}{k_2}\right)T_{j-1}^{k+1} + \frac{1}{k_1}T_{j+1}^{k+1}}{\frac{R_{1,2}}{\Delta x} + \frac{1}{k_1} + \frac{1}{k_2}} \tag{6}$$

$$T_{j^*}^{k+1} = \frac{\left(1 + \frac{\Delta x}{R_{1,2}k_1}\right)T_{j+1}^{k+1} + \frac{\Delta x}{R_{1,2}k_2}T_{j-1}^{k+1}}{1 + \frac{\Delta x}{R_{1,2}k_1} + \frac{\Delta x}{R_{1,2}k_2}} = \frac{\left(\frac{R_{1,2}}{\Delta x} + \frac{1}{k_1}\right)T_{j+1}^{k+1} + \frac{1}{k_2}T_{j-1}^{k+1}}{\frac{R_{1,2}}{\Delta x} + \frac{1}{k_1} + \frac{1}{k_2}} \tag{7}$$

Eqs. (6) and (7) indicate that the temperatures at the two sides of the interface are dependent on the temperatures at the two nodes adjacent

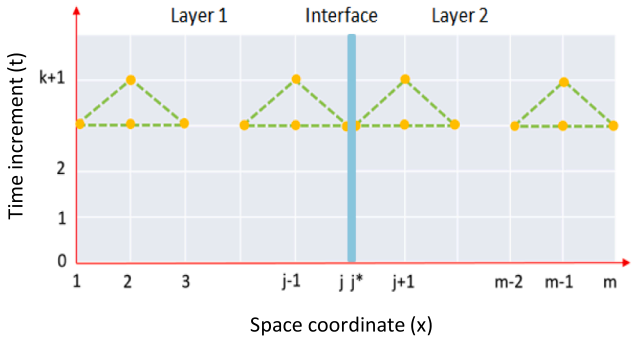

Fig. 1. Explicit scheme for calculation of temperature in one-dimensional two-layered composites with ITR at $x = x_j = x_{j^*}$.

to the interface, the thermal properties of the two layers surrounding the interface, and the thermal resistance of the interface itself. Finally, the temperature at the two boundaries where $x = 0$ and $x = x_m$ can be determined based on the prescribed boundary conditions. For example, if the temperature and heat flux are prescribed at $x = 0$ and $x = x_m$, respectively, then the corresponding temperatures there can be expressed as follows,

$$T_1^{k+1} = T_1 \quad \text{at} \quad x = 0 \tag{8}$$

$$T_m^{k+1} = T_{m-1}^{k+1} - \frac{q_m \Delta x}{k_2} \quad \text{at} \quad x = x_m \tag{9}$$

where T_1 and q_m are the prescribed temperature and heat flux applied on the surfaces at $x = 0$ and $x = x_m$, respectively. The temperatures given by Eqs. (4)–(9) are the solution obtained by using the finite difference method. Also, it should be noted that the explicit time-integration scheme is not unconditionally stable. Thus, when Eqs. (4)–(9) are employed smaller time steps should be used in the calculations in order to achieve accurate results.

3. Virtual layer representing discontinuity condition of temperature at interfaces

To describe the discontinuity condition of temperature at the interface in a two-layered composite, herein a virtual layer model is proposed to represent the interface. Thus, the original two-layered composite with ITR shown in Fig. 2a is now represented by the three-layered composite shown in Fig. 2b, in which the middle layer represents the interface (virtual layer) which reflects the ITR in the two-layered composite. Since the virtual layer could be very thin it would be reasonable to assume the temperature to be linearly distributed in the virtual layer. According to the continuity condition of heat flux at each side of the virtual layer, the following two equations can be obtained,

$$k_1 \frac{T_j^{k+1} - T_{j-1}^{k+1}}{\Delta x} = k_{int} \frac{T_{j^*}^{k+1} - T_j^{k+1}}{\Delta x_{int}} \tag{10}$$

$$k_2 \frac{T_{j+1}^{k+1} - T_{j^*}^{k+1}}{\Delta x} = k_{int} \frac{T_{j^*}^{k+1} - T_j^{k+1}}{\Delta x_{int}} \tag{11}$$

where k_{int} is the thermal conductivity coefficient of the virtual layer and $\Delta x_{int} = x_{j^*} - x_j$ is the thickness of the virtual layer. The energy conservation in the virtual layer requires the following equation:

$$(\rho_{int} c_{int}) \frac{\partial T_{int}}{\partial t} = -\frac{\partial}{\partial n}\left(k_2 \frac{\partial T_2}{\partial n} + k_1 \frac{\partial T_1}{\partial n}\right) \tag{12}$$

where ρ_{int} and c_{int} are the density and specific heat of the virtual layer, respectively, and T_{int} is the temperature in the virtual layer. According to the flux expressions given by Eqs. (10) and (11), it can be concluded that the right-hand-side of Eq. (12) is zero. This indicates that if a linear temperature distribution is assumed in the virtual layer then the specific heat or the density of the virtual layer must be zero, i.e. $c_{int} = 0$ or $\rho_{int} = 0$. Eqs. (10) and (11) can be also used to solve for the temperatures at the two sides of the virtual layer, which yields,

$$T_j^{k+1} = \frac{\left(1 + \frac{\Delta x k_{int}}{\Delta x_{int} k_2}\right) T_{j-1}^{k+1} + \frac{\Delta x k_{int}}{\Delta x_{int} k_1} T_{j+1}^{k+1}}{1 + \frac{\Delta x k_{int}}{\Delta x_{int} k_1} + \frac{\Delta x k_{int}}{\Delta x_{int} k_2}} = \frac{\left(\frac{\Delta x_{int}}{\Delta x k_{int}} + \frac{1}{k_2}\right) T_{j-1}^{k+1} + \frac{1}{k_1} T_{j+1}^{k+1}}{\frac{\Delta x_{int}}{\Delta x k_{int}} + \frac{1}{k_1} + \frac{1}{k_2}} \tag{13}$$

$$T_{j^*}^{k+1} = \frac{\left(1 + \frac{\Delta x k_{int}}{\Delta x_{int} k_1}\right) T_{j+1}^{k+1} + \frac{\Delta x k_{int}}{\Delta x_{int} k_2} T_{j-1}^{k+1}}{1 + \frac{\Delta x k_{int}}{\Delta x_{int} k_1} + \frac{\Delta x k_{int}}{\Delta x_{int} k_2}} = \frac{\left(\frac{\Delta x_{int}}{\Delta x k_{int}} + \frac{1}{k_1}\right) T_{j+1}^{k+1} + \frac{1}{k_2} T_{j-1}^{k+1}}{\frac{\Delta x_{int}}{\Delta x k_{int}} + \frac{1}{k_1} + \frac{1}{k_2}} \tag{14}$$

Comparing Eqs. (13) and (14) with Eqs. (6) and (7), one can find that, if k_{int} is chosen as $k_{int} = \Delta x_{int}/R_{1,2}$, then the temperatures at the two sides of the interface calculated from Eqs. (6) and (7) are exactly the same as the temperatures at the two sides of the virtual layer calculated from Eqs. (13) and (14). This means that if the virtual layer with thickness Δx_{int}, thermal conductivity coefficient $k_{int} = \Delta x_{int}/R_{1,2}$ and zero specific heat $c_{int} = 0$ or zero density $\rho_{int} = 0$ are used to represent the interface, then the results obtained from the three-layered composite without ITR will be effectively the same as those obtained from the two-layered composite with ITR. While the virtual layer is employed, both the temperature and heat flux will be continuous at the two interfaces between layer 1 and virtual layer and between layer 2 and virtual layer.

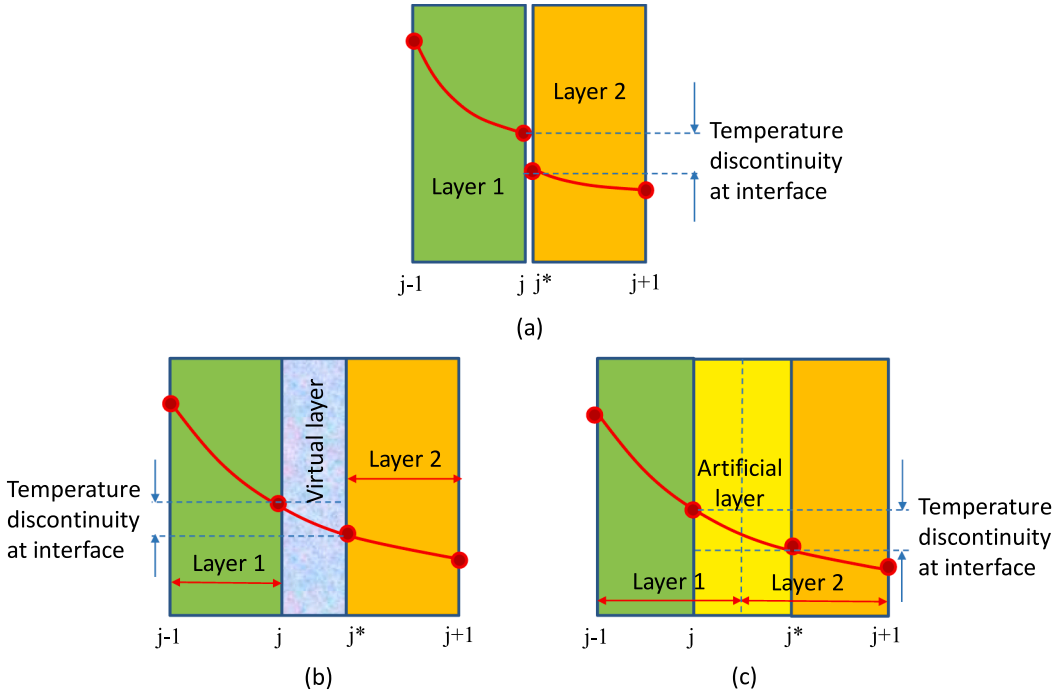

Fig. 2. Temperature distributions in different models. (a) Two-layered composite with ITR. (b) Virtual layer model. (c) Artificial layer model.

The benefit of using the virtual layer to model the interface with ITR is its convenience when the problem is solved by using the finite element method as it does not need to use special interface element to reflect the effect of ITR.

4. Artificial layer representing discontinuity condition of temperature at interfaces

The weakness of using the virtual layer is the need to modify the domain of the structure to be analysed. To avoid this problem, an alternative approach is to overlay the virtual layer to the existing materials in the two sides of the interface. For example, a half of its thickness is overlaid in layer 1 and the other half is overlaid in layer 2 (see Fig. 2c) to create an artificial layer Δx, which consists of three different materials that are connected in series. The thermal properties of the artificial layer thus can be expressed as follows,

$$\rho_{eff}c_{eff} = \frac{1}{2}(\rho_1 c_1 + \rho_2 c_2) \tag{15}$$

$$\frac{1}{k_{eff}} = \frac{1}{k_{int}} + \frac{1}{2k_1} + \frac{1}{2k_2} \tag{16}$$

where ρ_{eff}, c_{eff} and k_{eff} are the effective density, effective specific heat and effective thermal conductivity coefficient of the artificial layer, respectively, $k_{int} = \Delta x/R_{1,2}$, and Δx is the width of the artificial layer. The temperatures at node j and j* thus can be calculated by using Eq. (1), as follows,

$$T_j^{k+1} = T_j^k + \left(\frac{k_1}{\rho_1 c_1}\right)\left(\frac{\Delta t}{\Delta x^2}\right)\left[\frac{k_{eff}}{k_1}\left(T_{j^*}^k - T_j^k\right) - \left(T_j^k - T_{j-1}^k\right)\right] \tag{17}$$

$$T_{j^*}^{k+1} = T_{j^*}^k + \left(\frac{k_2}{\rho_2 c_2}\right)\left(\frac{\Delta t}{\Delta x^2}\right)\left[\left(T_{j+1}^k - T_{j^*}^k\right) - \frac{k_{eff}}{k_2}\left(T_{j^*}^k - T_j^k\right)\right] \tag{18}$$

As a numerical example, Fig. 3 shows a comparison of the temperature profiles at the time of t = 0.417 h in a two-layer composite plate, each layer has 0.5 m thickness, and the ITR is $R_{int} = 1/500$ m^2·K/W. The results plotted in Fig. 3 are obtained by using (1) the finite difference method for the actual two-layer model with ITR as described in Section 2, (2) the finite element method for the virtual layer model described in Section 3, and (3) the finite element method for the artificial layer model described in this Section. The thermal properties of the composite plate used in the example are given in Table 1. The initial temperature of the composite plate is assumed to be 20 °C. The temperatures of the composite plate at its two sides are assumed to be 480 °C and 20 °C, respectively. The thicknesses of the virtual layer and artificial layer are taken as $\Delta x_{\text{int}} = \Delta x = 0.02$ m. Note that the total thickness of the two-layer composite plate is 1.0 m in both the actual two-layer model and artificial layer model; whereas in the virtual layer model it is $1 + \Delta x_{\text{int}} =$ 1.02 m (0.02 m is the thickness of the virtual layer). For the presentation of comparison, the temperature profile in the virtual layer model plots only the temperature in layer 1 and layer 2 (i.e. the temperature in the virtual layer has been narrowed down to a point), so that the total thickness in the plot keeps the same as that in the other two models; whereas the actual variation of the temperature in the virtual layer is plotted in the zoom plot of the figure to visualise its variation.

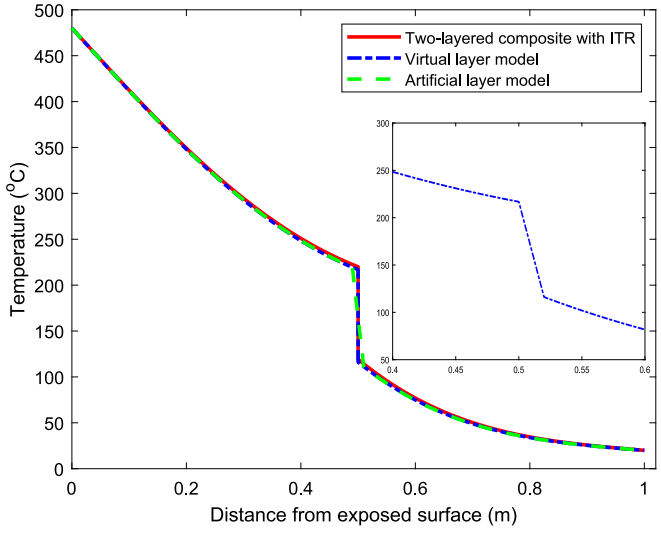

Fig. 3. Comparison of temperature profiles at t = 0.417 hrs in a two-layer composite plate with ITR $R_{int} = 1/500$ m^2·K/W obtained from three different models. The zoom plot shows the temperature variation in the virtual layer, which is not shown in the main plot.

It can be seen from Fig. 3 that the temperature profiles given by the actual two-layer model with ITR and the virtual layer model are almost identical, which demonstrates that the use of virtual layer model to analyse the heat transfer in multi-layered composites is reliable and able to provide accurate results. The temperature predicted by the artificial layer model is also almost the same as that calculated by the actual two-layer model with ITR, except for those in the artificial layer where the temperature drops continuously from layer 1 to layer 2, instead of a jump at the interface. This means that if the thickness of the artificial layer is sufficient small then the artificial layer model can also provide accurate temperature distribution.

Fig. 4 shows the comparison of temperature histories at the two sides of the interface, obtained from the three models. The figure demonstrates the ability of the virtual layer model which is able to provide accurate results; whereas the results provided by the artificial layer model are approximate, the accuracy of which is dependent on the thickness of the artificial layer employed in the model. The temperature histories plotted in Fig. 4 show that under the influence of ITR the temperature jump at the interface between layers 1 and 2 increases with time.

5. Heat transfer analysis of composites with multilayer coatings involving ITR

TBCs are the advanced materials that are usually used as coatings on turbines, aircraft engines and structural components for materials protection against excessive heat in high-temperature processes [6,27,28]. TBCs are often made by using multi-layered composites with several different materials in order to perform well in aggressive thermo-mechanical environments. ITR is normally generated in such multi-layer coatings to provide thermal barrier. Depending on the type of applications, the thickness of TBCs can be in the range from nanometres to millimetres. Owing to the significant scale difference between the coating and substrate, the heat transfer analysis for such composites need to use special finite element methods or multi-scale models [29–33]. However, if the present virtual layer model is used, the analysis would be much simple. Here, as an example, we consider the heat transfer in an aluminium plate (substrate) coated with a multi-layer polymer metal laminate (PML) on its rear surface. The thicknesses and thermal properties of the aluminium and PML are taken directly from [34] and given in Table 2. In the experiment the aluminium plate is subjected to a constant heat flux of 50 kW/m^2 on its uncoated front

Table 1
Thermal properties used in example 1.

Layer	Thickness (m)	Density (kg/m^3)	Specific heat (J/(kg·K))	Thermal conductivity (W/(m·K))
1	0.5	2700	1000	200
2	0.5	2700	1000	100
Virtual	0.02	0	0	10
Artificial	0.02	2700	1000	9.95

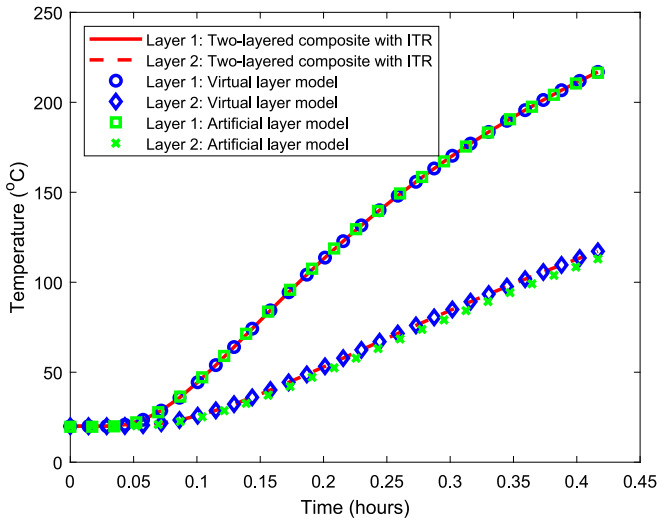

Fig. 4. Comparison of time-histories of temperatures at two sides of interface in a two-layer composite plate with ITR $R_{int} = 1/500$ m^2·K/W obtained from three different models.

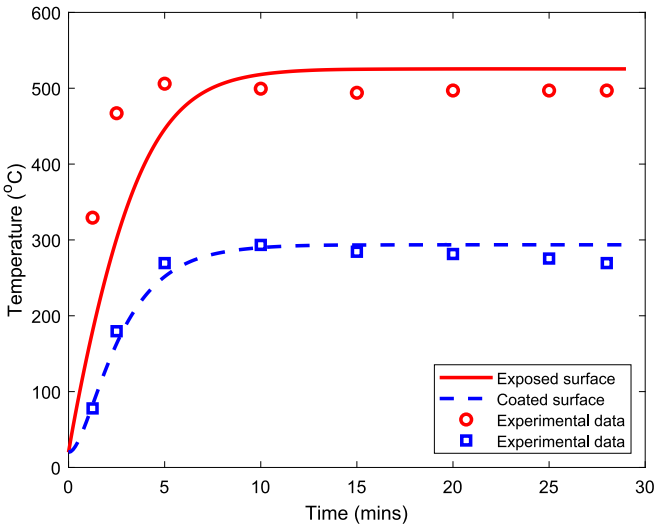

Fig. 5. Time-histories of temperature on the front and rear surfaces of coated aluminium plate (lines are prediction and symbol-points are experimental data from [34]).

Table 2
Thermal properties of aluminium with PML coating used in example 2.

Layer	Thickness (mm)	Density (kg/m^3)	Specific heat (J/(kg·K))	Thermal conductivity (W/(m·K))
Aluminium	6.35	2700	900	121
PML	0.8	2450	1000	1.09

surface and exposed to room temperature on its coated rear surface. The boundary conditions of the plate at the front and rear surfaces thus can be expressed as follows,

$$-k_1\frac{\partial T}{\partial x} = q - h_1(T-20) - \sigma\varepsilon_1\left[(T+273)^4 - 293^4\right] \tag{19}$$

$$k_2\frac{\partial T}{\partial x} = -h_2(T-20) - \sigma\varepsilon_2\left[(T+273)^4 - 293^4\right] \tag{20}$$

where k_1 and k_2 are the thermal conductivity coefficient of the aluminium and PML, h_1 and h_2 are the convective coefficient of the front and rear surfaces, ε_1 and ε_2 are the surface emissivity of the front and rear surfaces, and $\sigma = 5.6704 \times 10^{-8}$ W/(m^2·K^4) is the Stefan-Boltzmann constant. In the present simulation, the ambient temperature is assumed to be 20 °C, $h_1 = 25$ W/(m^2·K) and $\varepsilon_1 = 0.75$ on the front surface exposed to heat flux, $h_2 = 9.0$ W/(m^2·K) and $\varepsilon_2 = 1.0$ on the rear surface exposed to ambient temperature are assumed herein since these parameters are not available in [34]. The ITR between the substrate and coating layer is assumed to be $R_{int} = 1/50$ m^2·K/W. Considering the lateral flow of heat on the front surface the actual heat flux used in Eq. (19) is reduced by a factor of 0.75, that is $q = 0.75 \times 50$ kW/m^2.

Fig. 5 shows the time histories of the temperature on the front and rear surfaces of the coated aluminium plate obtained from the present virtual layer model (lines) and tests [34] (points), respectively. In the virtual layer model the thickness of the virtual layer is assumed to be $\delta =$ 0.01 mm. It can be seen from the figure that the temperatures on the both sides increase with time initially very quick; but with the increase of time they become stabilized, which means that the heat flux into the plate from the front surface is almost balanced by the heat flux out from the plate on the rear surface. It is evident from Fig. 5 that the predictions are in very good agreement with those obtained from the experiments. To demonstrate the importance of considering ITR in the heat transfer model, Fig. 6 shows the temperature profiles at three different times obtained from the virtual layer model. It can be observed from the figure

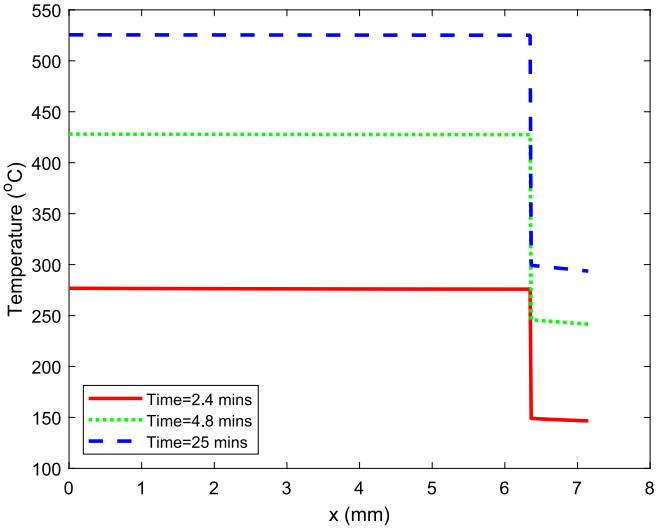

Fig. 6. Temperature distribution profiles in coated aluminium plate at different times.

that the temperature has very small variation in either the substrate layer or the coating layer. In contrast, the temperature jump at the interface is very significant. Therefore, it would be expected that, if the ITR were ignored the temperature at the rear surface of the plate would be very high. This implies that the thermal barrier in the multilayer coatings is mainly provided by the ITR rather than by the materials of the coatings.

For a thin multilayer coating with ITR, its effect on the heat transfer into the coated substrate can be modelled by using a modified surface boundary condition. Consider a substrate with a bilayer surface coating as shown in Fig. 7. It is assumed that ITR exists only at the interface between coating layers 1 and 2, but not at the interface between coating layer 2 and substrate. Since the thicknesses of the coating layers 1 and 2 are much smaller than that of the substrate, the temperature in these two coating layers can be assumed to be linearly distributed as plotted in Fig. 7. According to the continuity condition of heat flux, the following equations can be established,

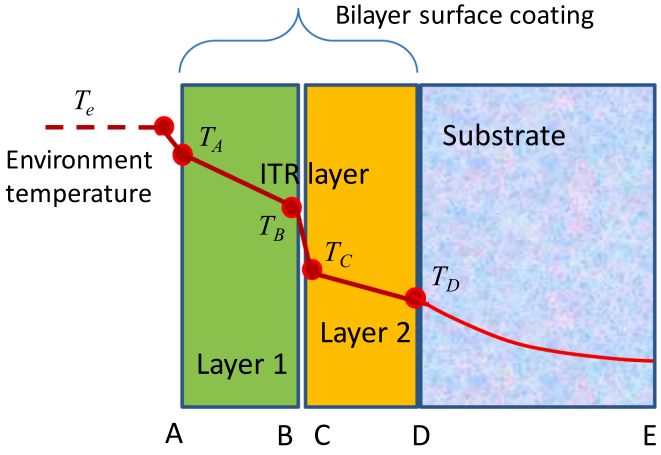

Fig. 7. Temperature distribution in a composite with bilayer surface coatings.

$$h_b(T_e - T_A) = \frac{k_1}{\Delta_1}(T_A - T_B) \tag{21}$$

$$\frac{k_1}{\Delta_1}(T_A - T_B) = \frac{1}{R_{12}}(T_B - T_C) \tag{22}$$

$$\frac{1}{R_{12}}(T_B - T_C) = \frac{k_2}{\Delta_2}(T_c - T_D) \tag{23}$$

$$\frac{k_2}{\Delta_2}(T_c - T_D) = -k_s\frac{\partial T_D}{\partial x} \tag{24}$$

where h_b is the convective coefficient of the exposed surface, k_1 and k_2 are the thermal conductivity coefficient of the coating layers 1 and 2, Δ_1 and Δ_2 are the thickness of the coating layers 1 and 2, R_{12} is the thermal resistance of the interface between coating layers 1 and 2, k_s is the thermal conductivity coefficient of the substrate, T_e, T_A, T_B, T_C, and T_D are the temperatures in the environment next to the coated surface, on the two sides of layer 1 and layer 2 (see Fig. 7), respectively. If the surface radiation on the exposed surface is involved, then h_b will be the function of temperature T_e and T_A. Solving Eqs. (20)–(23) for T_A, T_B, T_C, and T_D, it yields,

$$T_D = T_e + k_s\left(\frac{1}{h_b} + \frac{\Delta_1}{k_1} + R_{12} + \frac{\Delta_2}{k_2}\right)\frac{\partial T_D}{\partial x} \tag{25}$$

$$T_C = T_e + k_s\left(\frac{1}{h_b} + \frac{\Delta_1}{k_1} + R_{12}\right)\frac{\partial T_D}{\partial x} \tag{26}$$

$$T_B = T_e + k_s\left(\frac{1}{h_b} + \frac{\Delta_1}{k_1}\right)\frac{\partial T_D}{\partial x} \tag{27}$$

$$T_A = T_e + k_s\left(\frac{1}{h_b}\right)\frac{\partial T_D}{\partial x} \tag{28}$$

Use Eq. (26) to substitute T_c in Eq. (24), yielding,

$$h_{eff}(T_e - T_D) = -k_s\frac{\partial T_D}{\partial x} \tag{29}$$

in which,

$$h_{eff} = \frac{1}{\frac{1}{h_b} + \frac{\Delta_1}{k_1} + R_{12} + \frac{\Delta_2}{k_2}} \tag{30}$$

This implies that if an effective convective coefficient h_{eff} is used, then the boundary condition of the temperature on the substrate surface can be expressed directly in terms of Eq. (29) where h_{eff} is defined by Eq. (30). Physically, Eq. (30) indicates that the thermal resistances provided by the interphase between the environment and exposed surface of coating layer 1, the materials of coating layers 1 and 2, and the ITR of the interface between coating layers 1 and 2 can be calculated by using the in-series model, which is similar to that reported in literature [6,16,19,35]. By using Eqs. (29) and (30) as the boundary condition of the substrate one can avoid the modelling of the multilayer surface coatings. In other words, the effect of the multilayer coatings on the heat transfer in the substrate can be simplified by modifying its exposed boundary condition given by Eq. (29).

It should be noted that, although only one-dimensional problems are discussed in the present study, the two models developed above can be easily extended to two- and three-dimensional problems where the virtual layer or artificial layer will turn into the virtual element or artificial element. However, owing to the large scale difference in the geometry, the corresponding virtual element or artificial element has to be treated as the orthotropic material. The thermal conductivity derived in the present study can be used as the thermal conductivity in the direction normal to the interface, whereas the interface-contributed heat transfer in the directions parallel to the interface could generally be ignored in the virtual element or artificial element. In other words, as far as the interface element is concerned the heat transfer takes place only in the direction normal to the interface regardless of the dimension of the problem. Also, it should be mentioned here that, the experimental measurement of ITR is very difficult and the reported data on ITR are sparse as a result of a lack of efficient measurement methods [36]. In literature ITR are mostly determined by using the combination of analytical and measurement methods.

6. Conclusions

This paper has presented two one-dimensional heat transfer analysis models to deal with the ITR involved in multi-layered composites. The models can describe accurately the effect of ITR on the heat transfer in composites and are easily implemented in the finite element analysis models. From the results obtained in the present study the following conclusions can be drawn.

- The thermal resistance generated by an interface in multi-layered composites can be modelled by using the virtual layer model or the artificial layer model. The former involves the interface only, whereas the latter includes not only the interface but also parts of the materials in the layers surrounding the interface.
- In the virtual layer model, the density or specific heat assigned to the virtual layer should be taken as zero; whereas the thermal conductivity coefficient of the virtual layer should be equal to the thickness of the virtual layer divided by the thermal resistance of the interface.
- In the artificial layer model, the thermal properties assigned to the artificial layer should use their effective thermal properties. The effective density and effective specific heat are calculated based on the concept of volume average; whereas the effective thermal conductivity coefficient is determined based on the in-series model.

Declaration of Competing Interest

The authors declare that they have no known competing financial interests or personal relationships that could have appeared to influence the work reported in this paper.

Acknowledgment

The work presented in the paper was supported by the National Natural Science Foundation of China (grant No. 52078300).

References

[1] Chen ZL, Li JC, Sun LF, Li LY. Flexural buckling of sandwich beams with thermal-induced non-uniform sectional properties. J Build Eng 2019;25:100782.

[2] Gürdal Z, Haftka RT, Hajela P. Design and Optimization of Laminated Composite Materials. Oxford: Wiley; 1999. ISBN 978-0471252764.
[3] Bull SJ, Jones AM. Multilayer coatings for improved performance. Surf Coat Technol 1996;78(1-3):173–84.
[4] Viswanathan V, Dwivedi G, Sampath S. Multilayer, multimaterial thermal barrier coating systems: design, synthesis, and performance assessment. J Am Ceram Soc 2015;98(6):1769–77.
[5] Srivastava A, Joshi V, Shivpuri R, Bhattacharya R, Dixit S. A multilayer coating architecture to reduce heat checking of die surfaces. Surf Coat Technol 2003;163-164:631–6.
[6] Josell D, Bonevich JE, Nguyen TM, Johnson RN. Heat transfer through nanoscale multilayered thermal barrier coatings at elevated temperatures. Surf Coat Technol 2015;275:75–83.
[7] Kovalev AI, Rashkovskiy AY, Wainstein DL, Gago R, Soldera F, Endrino JL. Influence of electronic structure, plasmon-phonon and plasmon-polariton excitations on anomalously low heat conductivity in TiAlN/Ag nanoscale multilayer coatings. Curr Appl Phys 2016;16(4):459–68.
[8] Tang WZ, Yang L, Zhu W, Zhou YC, Guo JW, Lu C. Numerical simulation of temperature distribution and thermal-stress field in a turbine blade with multilayer-structure TBCs by a fluid–solid coupling method. J Mater Sci Technol 2016;32(5):452–8.
[9] Liu JH, Liu YB, He X, Liu L. Study on TBCs insulation characteristics of a turbine blade under serving conditions. Case Stud Therm Eng 2016;8:250–9.
[10] Zhu W, Wang JW, Yang L, Zhou YC, Wei YG, Wu RT. Modeling and simulation of the temperature and stress fields in a 3D turbine blade coated with thermal barrier coatings. Surf Coat Technol 2017;315:443–53.
[11] Sun X, Dong X, Wang K, Wang R, Fan Z, Duan W. Experimental investigation on thermal effects in picosecond laser drilling of thermal barrier coated In718. Opt Laser Technol 2019;113:150–8.
[12] Ge WA, Zhao CY, Wang BX. Thermal radiation and conduction in functionally graded thermal barrier coatings. Part I: Experimental study on radiative properties. Int J Heat Mass Transf 2019;134:101–13.
[13] Munuhe TW, Chen R-H, Zhu L, Ma R. Modeling molten droplet spreading and infiltration into non-isothermal thermal barrier coatings. Int J Heat Mass Transf 2022;182:121942.
[14] Ruan K, Shi X, Guo Y, Gu J. Interfacial thermal resistance in thermally conductive polymer composites: A review. Compos Commun 2020;22:100518. https://doi.org/10.1016/j.coco.2020.100518.
[15] Feng C-P, Yang L-Y, Yang J, Bai Lu, Bao R-Y, Liu Z-Y, et al. Recent advances in polymer-based thermal interface materials for thermal management: A mini-review. Compos Commun 2020;22:100528. https://doi.org/10.1016/j.coco.2020.100528.
[16] Choi HK, Jung H, Oh Y, Hong H, Yu J, Shin ES. Analysis of the influence of interphase characteristics on thermal conduction in surface-modified carbon nanotube-reinforced composites using an analytical model. Compos Sci Technol 2018;168:145–51.
[17] Choi HK, Jung H, Oh Y, Hong H, Yu J, Shin ES. Interfacial effects of nitrogen-doped carbon nanotubes on mechanical and thermal properties of nanocomposites: A molecular dynamics study. Compos B Eng 2019;167:615–20.
[18] Hassanzadeh-Aghdam MK, Mahmoodi MJ, Jamali J. Effect of CNT coating on the overall thermal conductivity of unidirectional polymer hybrid nanocomposites. Int J Heat Mass Transf 2018;124:190–200.
[19] Fang Y, Li LY, Mawulé Dassekpo JB, Jang SH. Heat transfer modelling of carbon nanotube reinforced composites. Compos B Eng 2021;225:109280.
[20] Yan SL, Li LY. Finite element analysis of cyclic indentation of an elastic-perfectly plastic half-space by a rigid sphere. J Mech Eng Sci 2003;217(5):505–14.
[21] Zhong HL, Lukes JR. Interfacial thermal resistance between carbon nanotubes: molecular dynamics simulations and analytical thermal modelling. Phys Rev B 2006;74(12):125403.
[22] Kapitza PL. Heat transfer and superfluidity of helium II. Phys Rev J Arch 1941;60(4):354–5.
[23] Stoner RJ, Maris HJ. Kapitza conductance and heat flow between solids at temperatures from 50 to 300 K. Phys Rev B 1993;48(22):16373–87.
[24] Lyeo HK, Cahill DG. Thermal conductance of interfaces between highly dissimilar materials. Phys Rev B 2006;73:144301.
[25] Dechaumphai E, Lu D, Kan JJ, Moon J, Fullerton EE, Liu Z, et al. Ultralow thermal conductivity of multilayers with highly dissimilar Debye temperatures. Nano Lett 2014;14(5):2448–55.
[26] Wang L, Zhong XH, Zhao YX, Yang JS, Tao SY, Zhang W, et al. Effect of interface on the thermal conductivity of thermal barrier coatings: A numerical simulation study. Int J Heat Mass Transf 2014;79:954–67.
[27] Han X, Huang Y, Peng X, Gao X, Li T, Liu P. 3D continuous copper networks coated with graphene in Al-matrix composites for efficient thermal management. Compos Struct 2021;258:113177.
[28] Zhang T, Xi J, Qiu S, Zhang B, Luo Z, Xing W, et al. Facilely produced highly adhered, low thermal conductivity and non-combustible coatings for fire safety. J Colloid Interface Sci 2021;604:378–89.
[29] She Z, Wang K, Li P. Thermal analysis of multilayer coated fiber-reinforced composites by the hybrid Trefftz finite element method. Compos Struct 2019;224:110992.
[30] Nguyen CH, Chandrashekhara K, Birman V. Multifunctional thermal barrier coating in aerospace sandwich panels. Mech Res Commun 2012;39(1):35–43.
[31] Li L-Y, Bettess P, Bull JW, Bond T, Applegarth I. Theoretical formulations for adaptive finite element computations. Commun Numer Methods Eng 1995;11(10):857–68.
[32] Tian L, Wang G, Zhao H, Yuan M, Peng Y, Chen J. A novel multiscale semi-analytical approach for thermal properties of fuzzy fiber reinforced composites. Compos Struct 2021;275:114424.
[33] Zhou LiChuan, Sun XiaoHao, Chen MingWei, Zhu YinBo, Wu HengAn. Multiscale modeling and theoretical prediction for the thermal conductivity of porous plain-woven carbonized silica/phenolic composites. Compos Struct 2019;215:278–88.
[34] Christke S, Gibson AG, Grigoriou K, Mouritz AP. Multi-layer polymer metal laminates for the fire protection of lightweight structures. Mater Des 2016;97:349–56.
[35] Duan HL, Yi X, Huang ZP, Wang J. A unified scheme for prediction of effective moduli of multiphase composites with interface effects. Part I: theoretical framework. Mech Mater 2007;39(1):81–93.
[36] Xu Y, Wang H, Tanaka Y, Shimono M, Yamazaki M. Measurement of interfacial thermal resistance by periodic heating and a thermo-reflectance technique. Mater Trans 2007;48(2):148–50.